For the $c_{pa} = 0.10$ treatment the Liapunov exponent is 0, which is consistent with a quasiperiodic attractor that forms an invariant loop in phase space. In the $c_{pa} = 0.25$ and $c_{pa} = 0.35$ treatments, the Liapunov exponent is positive and the attractors are chaotic. A region of multiple attractors (chaos and 3-cycles) is associated with the $c_{pa} = 0.50$ treatment. The stochastic variability of larvae and adults in the c_{pa}-manipulated treatments was larger than that of the unmanipulated control treatment as measured by the estimated noise variances (main diagonal in the Σ matrices) (*15*).

Despite the effects of stochasticity, which are always present in experimental populations, a close examination of the data reveals features of the predicted deterministic attractors. The time-series data for one replicate culture of each experimental treatment are given in Fig. 2. Comparison with the control shows that the experimental manipulations had a destabilizing effect on the population dynamics. For the control cultures, the model forecasts an asymptotic approach to a stable equilibrium with slowly increasing adult numbers. For $c_{pa} = 0.0$, the model predicts an oscillatory approach to equilibrium, with approximately equal numbers of insects in all three life stages. For $c_{pa} = 1.0$, a distinctive 3-cycle is predicted, with a repeating high-low-low pattern. These predictions are supported by the data.

The complex deterministic attractors forecast for the remaining treatments are more clearly visualized in phase space. In this case, phase space is three-dimensional with state variables L_t, P_t, and A_t. However, because P_t is a constant multiple of L_{t-1}, the features of the attractors are adequately seen when projected onto the L_t-A_t plane.

Data points for all replicates of each treatment are plotted in the projected phase planes in Fig. 3. To deemphasize the presence of transients (and hence better discern the features of the asymptotic attractors), we omitted the first 10 data points in these plots. The control and $c_{pa} = 0.0$ treatments show tight clusters of data points, as is consistent with the model prediction of a stable equilibrium (with noise). The $c_{pa} = 0.0$ cluster is less tightly packed in phase space than is the control, reflecting the increased stochastic variability of the c_{pa}-manipulated cultures. The $c_{pa} = 0.05$ and $c_{pa} = 0.10$ treatments show different patterns of data points, which are consistent with the predicted invariant loops. In the $c_{pa} = 0.10$ plot, the invariant loop is displayed with the data; in the $c_{pa} = 0.05$ plot, the model forecasts period locking on the invariant loop with period 8, as shown. For $c_{pa} = 0.25$, the data are scattered around the predicted chaotic attractor, which consists of several islands of points. In the $c_{pa} = 0.35$ plot, the data are distributed in the L-A plane in a manner similar to the predicted chaotic attractor. For the treatments $c_{pa} = 0.50$ and $c_{pa} = 1.0$, the data are distributed tightly along the L and A axes, as predicted by the chaotic attractor and 3-cycles shown. A close examination of these plots reveals a clustering of the data around the displayed cycle points.

The experimental confirmation of nonlinear phenomena in the dynamics of the laboratory beetle lends credence to the hypothesis that fluctuations in natural populations might often be complex, low-dimensional dynamics produced by nonlinear feedbacks. In our study, complex dynamics were obtained by "harvesting" beetles to manipulate rates of adult mortality and recruitment. For applied ecology, the experiment suggests adopting a cautious approach to the management or control of natural populations, based on sound scientific understanding. In a poorly understood dynamical population system, human intervention—such as changing a death rate or a recruitment rate—could lead to unexpected and undesired results.

REFERENCES AND NOTES

1. M. P. Hassell and R. M. May, Eds., *Population Regulation and Dynamics* (Cambridge Univ. Press, Cambridge, 1990).
2. R. Pool, *Science* **243**, 310 (1989).
3. H. Tong and R. L. Smith, *J. R. Statist. Soc. B* **54**, 301 (1992).
4. H. C. J. Godfray and B. T. Grenfell, *Trends Ecol. Evol.* **8**, 43 (1993).
5. A. Hastings, C. L. Hom, S. Ellner, P. Turchin, H. C. J. Godfray, *Annu. Rev. Ecol. Syst.* **24**, 1 (1993).
6. S. Ellner and P. Turchin, *Am. Nat.* **145**, 343 (1995).
7. P. Kareiva, in *Perspectives in Ecological Theory*, J. Roughgarden, R. M. May, S. A. Levin, Eds. (Princeton Univ. Press, Princeton, NJ, 1989).
8. H. C. J. Godfray and S. P. Blythe, *Philos. Trans. R. Soc. London Ser. B* **330**, 221 (1990).
9. R. M. May, *Science* **186**, 645 (1974).
10. ——— and G. F. Oster, *Am. Nat.* **110**, 573 (1976).
11. Biologists have long used flour beetles of the genus *Tribolium* as a research tool to explore the dynamics of populations. The combination of high rates of reproduction, short life cycle (4 to 6 weeks from egg to adult), ease of culture, and a life history that includes strong nonlinear life-stage interactions (cannibalism) make the beetle a good laboratory system [A. Sokoloff, *The Biology of* Tribolium (Oxford Univ. Press, Oxford, 1972, 1974, 1977), vols 1 to 3); R. F. Costantino and R. A. Desharnais, *Population Dynamics and the* Tribolium *Model: Genetics and Demography* (Springer-Verlag, New York, 1991)].
12. B. Dennis, R. A. Desharnais, J. M. Cushing, R. F. Costantino, *Ecol. Monogr.* **65**, 261 (1995).
13. R. F. Costantino, J. M. Cushing, B. Dennis, R. A. Desharnais, *Nature* **375**, 227 (1995).
14. H. Tong, *Non-linear Time Series: A Dynamical System Approach* (Oxford Univ. Press, Oxford, 1990).
15. The maximum likelihood parameter estimates in the deterministic skeleton, estimated using all of the data, are $b = 6.598$, $c_{el} = 1.209 \times 10^{-2}$, $c_{ea} = 1.155 \times 10^{-2}$, and $\mu_l = 0.2055$. Using only the control cultures, we also obtained $c_{pa} = 4.700 \times 10^{-3}$ and $\mu_a = 7.629 \times 10^{-3}$, where μ_a was estimated directly from numbers of dead adults. The maximum likelihood estimates in the variance-covariance matrices are $\sigma_{11} = 0.3412$, $\sigma_{22} = 0.2488$, $\sigma_{33} = 1.627 \times 10^{-4}$, $\sigma_{12} = 7.312 \times 10^{-2}$, $\sigma_{13} = -1.719 \times 10^{-3}$, and $\sigma_{23} = 3.374 \times 10^{-4}$ for Σ-control, and $\sigma_{11} = 0.7731$, $\sigma_{22} = 0.1085$, $\sigma_{33} = 0.1031$, $\sigma_{12} = -1.262 \times 10^{-2}$, $\sigma_{13} = -4.638 \times 10^{-2}$, and $\sigma_{23} = 5.113 \times 10^{-3}$ for Σ-manipulated.
16. A. A. Berryman and J. A. Millstein, *Trends Ecol. Evol.* **4**, 26 (1989).

17. Supported in part by NSF grants DMS-9306271, DMS-9319073, DMS-9625576, and DMS-9616205.

14 August 1996; accepted 22 October 1996

A Mouse Model with Features of Familial Combined Hyperlipidemia

Lori Masucci-Magoulas, Ira J. Goldberg, Charles L. Bisgaier, Humaira Serajuddin, Omar L. Francone, Jan L. Breslow, Alan R. Tall*

Familial combined hyperlipidemia (FCHL) is a common inherited lipid disorder, affecting 1 to 2 percent of the population in Westernized societies. Individuals with FCHL have large quantities of very low density lipoprotein (VLDL) and low density lipoprotein (LDL) and develop premature coronary heart disease. A mouse model displaying some of the features of FCHL was created by crossing mice carrying the human apolipoprotein C-III (*APOC3*) transgene with mice deficient in the LDL receptor. A synergistic interaction between the apolipoprotein C-III and the LDL receptor defects produced large quantities of VLDL and LDL and enhanced the development of atherosclerosis. This mouse model may provide clues to the origin of human FCHL.

Familial combined hyperlipidemia is the most common genetic dyslipidemia and is characterized by large amounts of VLDL or LDL or both, as well as apolipoprotein B (APOB), and small amounts of high density lipoprotein (HDL) (*1*, *2*). FCHL affects about 5% of all individuals with coronary heart disease and 10% of individuals with

early-onset disease. FCHL is thought to be caused by an autosomal dominant gene with a primary effect on plasma triglyceride concentrations and a secondary effect on cholesterol concentrations (*1*, *3*). In one study of selected British families, FCHL was shown to be linked to the apolipoprotein A-I/apolipoprotein C-III/apolipoprotein A-IV (*A1/C3/A4*) gene cluster (*4*); other studies, although not confirming genetic linkage, have shown a strong association of FCHL with the *A1/C3/A4* (*5*) or lipoprotein lipase (*LPL*) genes (*6*). The genetic basis of FCHL remains unknown, however.

To create a mouse model of FCHL, we crossed mice carrying the human *APOC3* transgene, which have large quantities of VLDL (*7*), with mice carrying an inactive LDL receptor gene or a human *APOB* transgene, which have large quantities of LDL (*8*, *9*). The *APOC3* transgene markedly increased plasma VLDL and intermediate density lipoprotein (IDL) plus LDL (IDL-LDL) cholesterol when it was introduced into mice that were homozygously (LDLR0) or heterozygously (LDLR1) deficient for the LDL receptor (Fig. 1 and Table 1). The increase in IDL-LDL was more pronounced in mice fed the Western diet (three- to fourfold) than in those fed the chow diet (twofold). In addition, the *APOC3* transgene increased VLDL cholesterol concentrations tenfold in LDLR0 mice (both diets) and more than fivefold in LDLR1 mice. The human APOC3 transgenic mice used in this experiment had VLDL cholesterol concentrations less than 50 mg/dl and IDL-LDL cholesterol concentrations of 32 and 86 mg/dl when fed chow and Western diets, respectively (Table 1). Thus, the APOC3 and LDL receptor defects are synergistic, resulting in increased VLDL and IDL-LDL cholesterol. These results contrast with those observed when the human *APOC3* transgene was bred onto the human *APOB* transgene background where the effects on IDL-LDL and VLDL concentrations were less than additive (Table 1).

The *APOC3* transgene also increased plasma and VLDL triglyceride concentrations in the LDL receptor–deficient background (Table 1), but the magnitude of this effect was comparable with that observed in mice expressing the *APOC3* transgene alone (*7*). The *APOC3* transgene had the most pronounced effect on VLDL and IDL-LDL lipoprotein fractions and little effect on HDL. Because low HDL is a feature of FCHL, we introduced the human cholesteryl ester transfer protein (*CETP*) transgene into mice of various genetic backgrounds (*10*). Introduction of this gene onto the LDLR0/APOC3 background lowered HDL cholesterol by 79 and 36% in mice fed chow and Western diets, respectively (Fig. 1 and Table 1). It also resulted in redistribution of cholesterol from HDL and IDL-LDL to VLDL (Fig. 1 and Table 1) and of triglyceride from VLDL to IDL-LDL and HDL (*11*). Similar effects were observed in the LDLR1 mice. Mice have much higher LDL receptor activity than humans (*12*); thus, LDLR1 mice (on the Western diet) have IDL-LDL cholesterol concentrations similar to those of normolipidemic humans (80 to 100 mg/dl). The amounts of VLDL cholesterol (142 mg/dl) and IDL-LDL cholesterol (186 mg/dl) in LDLR1/APOC3/CETP mice are similar to those found in humans with FCHL (*1*, *2*). Thus, the combination of the human *APOC3* and *CETP* transgenes in the LDL receptor–deficient background produced a lipoprotein cholesterol profile resembling that of FCHL.

To determine whether the LDLR0/APOC3 mice showed the increased amounts of APOB that are characteristic of FCHL (*13*), we separated plasma lipoproteins by ultracentrifugation and analyzed them by SDS–polyacrylamide gel electrophoresis (SDS-PAGE). Overexpression of APOC3 in LDLR0 mice produced an increased content of APOB100 and APOB48 in IDL and, to a lesser extent, in VLDL, compared with the content in LDLR0 mice. Apolipoprotein E (APOE) content was increased in VLDL and IDL in the LDLR0/APOC3 mice; in contrast, APOE content in VLDL declined in

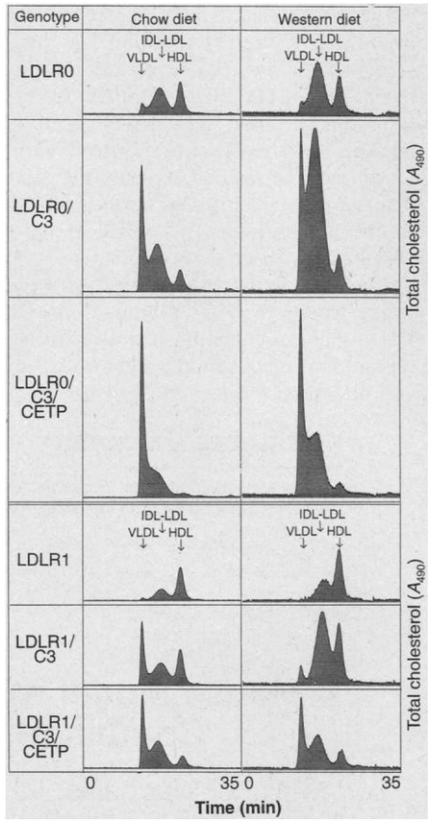

Fig. 1. Plasma lipoprotein cholesterol distribution in mice of different genotypes fed a Western (0.15% cholesterol, 20% saturated fat) or chow diet, as determined by high-performance gel filtration chromatography (*26*). Mice were obtained by cross breeding LDLR0 (*8*) with *APOC3* transgenic [line 3707, with moderate hypertriglyceridemia (*7*)] and NFR CETP transgenic [line 5203 (*10*)] mice. All mice were in a mixed genetic background (C57BL6/129), matched for sex (both male and female mice were studied), and 3 to 6 months old. LDLR0, homozygous LDL receptor gene knockout; LDLR0/C3, homozygous LDL receptor gene knockout/APOC3 transgenic; LDLR0/C3/CETP, homozygous LDL receptor gene knockout/cholesteryl ester transfer protein/APOC3 transgenic; LDLR1, heterozygous LDL receptor gene knockout; LDLR1/C3, heterozygous LDL receptor gene knockout/APOC3 transgenic; LDLR1/C3/CETP, heterozygous LDL receptor gene knockout/CETP/APOC3 transgenic.

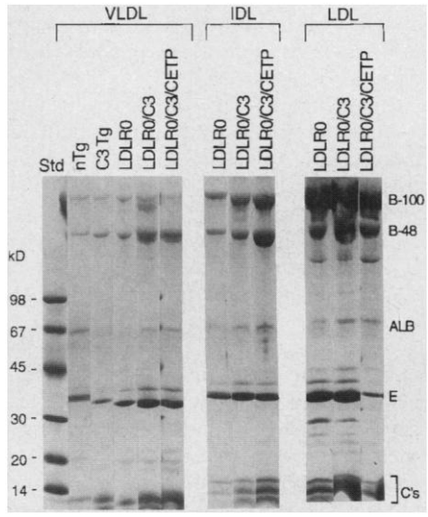

Fig. 2. SDS-PAGE analysis of the apolipoproteins of VLDL, IDL, and LDL fractions of mice of different genotypes after 3 months on the Western diet. VLDL [density (ρ) < 1.006 g/ml], IDL (1.006 < ρ < 1.019), and LDL (1.019 < ρ < 1.063) were separated from pooled plasma by ultracentrifugation in a Ti-100 ultracentrifuge, desalted, and concentrated; the final volume was normalized within each fraction. Each fraction (40 μl) was electrophoresed in a 3 to 20% polyacrylamide gel and proteins were detected by Coomassie blue staining. All mice (n = 6 to 10 per group) were matched for sex and age (3 to 6 months). nTg, nontransgenic littermates; Tg, transgenic; B-100, B-48, E, and C's, individual apolipoproteins; ALB, albumin.

L. Masucci-Magoulas, I. J. Goldberg, H. Serajuddin, A. R. Tall, Department of Medicine, Columbia University, 630 West 168 Street, New York, NY 10032, USA.
C. L. Bisgaier, Department of Vascular and Cardiac Diseases, Parke-Davis Pharmaceutical Research, 2800 Plymouth Road, Ann Arbor, MI 48105, USA.
O. L. Francone, Pfizer Inc., Central Research Division, Department of Metabolic Diseases, Eastern Point Road, Groton, CT 06340, USA.
J. L. Breslow, The Rockefeller University, Laboratory of Biochemical Genetics and Metabolism, 1230 York Avenue, New York, NY 10021, USA.
*To whom correspondence should be addressed.

Table 1. Total cholesterol (TC) and triglyceride (TG) concentrations in plasma and lipoproteins in different lines of transgenic mice. All values are milligrams per deciliter of plasma from a pool of at least six mice and are representative of samples obtained on two or three occasions. The integrated areas and percentage distribution from the high-performance gel filtration chromatography profiles (Fig. 1) were used to determine the total cholesterol concentration of each lipoprotein fraction (*26*). *APOC3* transgenic mice were line 3707 with moderate hypertriglyceridemia (*7, 13*). Littermates were matched for sex (both male and female mice were studied) and were 3 to 6 months old. Mice were fed the Western diet (0.15% cholesterol, 20% saturated fat) for 2 months except the LDLR1 and APOB transgenic groups, which were studied after 2 weeks on the diet.

Genotype	Cholesterol and triglyceride concentrations (mg/dl)									
	Chow diet		Western diet		Chow diet			Western diet		
	Plasma TC	Plasma TG	Plasma TC	Plasma TG	VLDL TC	IDL-LDL TC	HDL TC	VLDL TC	IDL-LDL TC	HDL TC
APOC3	124	783	201	956	49	32	43	35	86	80
LDLR0	221	241	403	107	18	121	78	20	288	95
LDLR0/C3	480	1625	1118	827	183	235	62	220	810	88
LDLR0/C3/CETP	429	1776	1105	1967	267	151	13	372	677	56
LDLR1	125	106	193	142	3	44	75	4	71	111
LDLR1/C3	269	920	451	466	82	103	84	24	284	136
LDLR1/C3/CETP	259	763	381	1415	103	126	30	142	186	56
APOB	114	192	245	249	4	70	40	4	116	124
APOB/C3	142	736	226	541	51	59	32	26	110	90

APOC3 transgenic mice (Fig. 2, C3 Tg VLDL) (*7*).

To ascertain whether the mice showed atherosclerosis susceptibility, we fed them a Western diet and measured the lesion area at the base of the aorta (Fig. 3). The lesion area in LDLR0/APOC3 mice was two to three times that in LDLR0 mice ($P < 0.0002$, t test). This contrasts with the situation in APOC3 transgenic mice, which do not show significant dietary atherosclerosis (*14*). Decreasing HDL by introducing the *CETP* transgene into the LDLR0/APOC3 background had no effect on lesion size. To investigate this unexpected result, we quantified the HDL subfractions in these mice by agarose electrophoresis. The pre-β but not the α subfraction of HDL (α-HDL) is thought to participate in reverse cholesterol transport (*15*). The HDL decrease produced by introduction of the *CETP* gene onto the LDLR0/APOC3 background was mainly in the α-HDL fraction (Table 2). This result may help explain why the HDL decrease did not enhance the development of atherosclerosis in the mice.

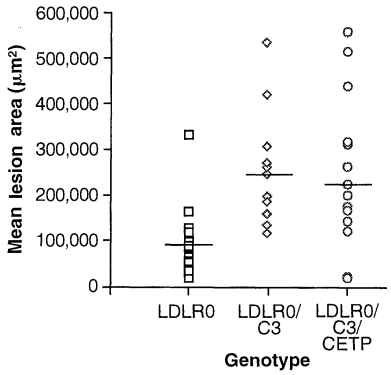

Fig. 3. Atherosclerotic lesion area in LDLR0, LDLR0/C3, and LDLR0/C3/CETP transgenic mice fed the Western diet for 3 months. Mean lesion area was determined in multiple sections of the proximal aorta by quantitation of intimal lipid accumulation from oil red O–stained sections (*27*). All groups of mice were matched for sex (both male and female mice were studied) and were 3 to 6 months old. There were at least 12 mice per group. Group means are indicated by horizontal bars. The level of significance was determined by t test of the natural logarithm of the mean lesion area. The mean lesion area in the LDLR0/C3 and LDLR0/C3/CETP mice was significantly increased compared with LDLR0 mice ($P < 0.0002$ and $P < 0.02$, respectively).

Our study suggests that genes, such as *APOC3*, that cause hypertriglyceridemia (increased VLDL) may be involved in the pathogenesis of FCHL. On the basis of transgenic mouse experiments, which showed that the expression of human or mouse *APOC3* transgenes, even at relatively low levels, caused hypertriglyceridemia, it has been proposed that overexpression of *APOC3* in humans may underlie hypertriglyceridemia (*7*). Several lines of evidence support this hypothesis. In clinical studies, two distinct haplotypes of the *A1/C3/A4* cluster—one characterized by the minor allele (X2) of an Xmn I restriction fragment length polymorphism (RFLP) 5′ to the gene complex and the other by the minor allele (S2) of an Sst I RFLP in the 3′ untranslated region of the *APOC3* gene—have been associated with hypertriglyceridemia (*5, 16–18*). One or two copies of the X2 allele are present in about 40% of patients with hypertriglyceridemia (*18*). The S2 allele, present in 40 to 50% of hypertriglyceridemic patients (*16*), is in strong linkage disequilibrium with polymorphisms in an insulin response element in the promoter of the *APOC3* gene (*19*). In cell culture studies, these polymorphisms render the *APOC3* gene insensitive to the normal insulin-mediated down-regulation of transcription. Further evidence that *APOC3* overexpression may underlie human hypertriglyceridemia comes from the finding that a hypotriglyceridemic class of drugs, the fibric acids, down-regulate *APOC3* transcription in the liver through a peroxisome proliferator–activated receptor-dependent mechanism (*20*).

The combined mouse and human data suggest that *APOC3* may be a common hypertriglyceridemia gene, which, in the proper setting of diminished LDL receptor activ-

Table 2. Distribution of APOA1 among pre–β-HDL and α-HDL in LDLR0, LDLR0/C3, and LDLR0/C3/CETP transgenic mice. Mice were fed the Western diet for 3 months. Pooled plasma from each group was quantitated. Values shown are means ± SD. Numbers in parentheses indicate number of mice per group. Lipoprotein fractions were separated by agarose gel electrophoresis and transferred to nitrocellulose membranes. Mouse APOA1 was detected with a rabbit polyclonal antibody. Areas containing pre–β-HDL and α-HDL were detected and quantitated with a PhosphorImager (Molecular Dynamics).

Genotype	APOA1 (mg/ml)	Percent of APOA1 in		Pre–β-HDL (mg/ml)
		Pre–β-HDL	α-HDL	
LDLR0 (5)	3.1 ± 0.75	16 ± 3	84 ± 3	0.50
LDLR0/C3 (4)	1.4 ± 0.20	33 ± 2	67 ± 2	0.46
LDLR0/C3/CETP (5)	0.6 ± 0.35	60 ± 11	40 ± 11	0.39

ity, can result in the FCHL phenotype. Although decreased LDL receptor activity is not thought to be the primary defect in human FCHL (*1*, *2*), LDL cholesterol and APOB amounts appear to be influenced by LDL receptor activity (*21*). In *APOC3* transgenic mice, hypertriglyceridemia arises from a delay in clearance of VLDL (*7*), reflecting an in vivo lipolysis defect (*7*, *22*), which may be caused by decreased binding of VLDL to endothelial cell proteoglycans, impairing access to LPL (*22*–*24*). It is possible that low LDL receptor activity results in increased conversion of accumulating VLDL into IDL and LDL. Other hypertriglyceridemia genes also might produce the FCHL phenotype. For example, deficiency of LPL activity has been found in some FCHL families (*6*, *25*). Although this is not usually because of alterations in the *LPL* gene itself (*25*), other genes that diminish LPL activity might underlie FCHL in some instances.

REFERENCES AND NOTES

1. J. L. Goldstein, H. G. Schrott, W. R. Hazzard, E. L. Bierman, A. G. Motulsky, *J. Clin. Invest.* **52**, 1544 (1973).
2. J. D. Brunzell *et al.*, *J. Lipid Res.* **24**, 147 (1983).
3. P. Cullen, B. Farren, J. Scott, M. Farrall, *Arterioscler. Thromb.* **14**, 1233 (1994).
4. A. P. Wojciechowski *et al.*, *Nature* **349**, 161 (1991). The genes for apolipoproteins A-I, C-III, and A-IV form a cluster on chromosome 11 [G. A. Bruns, S. K. Karathanasis, J. L. Breslow, *Arteriosclerosis* **4**, 97 (1984)]. These genes encode apoproteins involved in the formation and metabolism of VLDL and HDL.
5. C.-F. Xu *et al.*, *Clin. Genet.* **46**, 385 (1994).
6. S. P. Babirak *et al.*, *Arterioscler. Thromb.* **12**, 1176 (1992).
7. Y. Ito, N. Azrolan, A. O'Connell, A. Walsh, J. L. Breslow, *Science* **249**, 790 (1990); K. Aalto-Setälä *et al.*, *J. Clin. Invest.* **90**, 1889 (1992).
8. S. Ishibashi *et al.*, *J. Clin. Invest.* **92**, 833 (1994).
9. M. J. Callow, L. J. Stoltzfus, R. M. Lawn, E. M. Rubin, *Proc. Natl. Acad. Sci. U.S.A.* **91**, 2130 (1994); G. Chiesa *et al.*, *J. Clin. Invest.* **32**, 23747 (1993).
10. L. B. Agellon *et al.*, *J. Biol. Chem.* **266**, 10796 (1991); X.-C. Jiang, L. B. Agellon, A. Walsh, J. L. Breslow, A. R. Tall, *J. Clin. Invest.* **90**, 1290 (1992).
11. Analysis of the plasma lipoprotein triglyceride distribution by gel filtration chromatography showed an increase in IDL-LDL triglyceride (858 mg/dl) and HDL triglyceride (57 mg/dl) in LDLR0/C3/CETP mice compared with IDL-LDL triglyceride (350 mg/dl) and HDL triglyceride (10 mg/dl) in LDLR0/C3 mice.
12. J. M. Dietschy, S. D. Turley, D. K. Spady, *J. Lipid Res.* **34**, 1637 (1993).
13. S. Venkatesan, P. Cullen, P. Pacy, D. Halliday, J. Scott, *Arterioscler. Thromb.* **13**, 1110 (1993); J. D. Brunzell, A. D. Sniderman, J. J. Albers, P. O. Kwiterovich Jr., *Arteriosclerosis* **4**, 79 (1984).
14. T. Hayek *et al.*, *J. Clin. Invest.* **96**, 2071 (1995).
15. C. J. Fielding and P. E. Fielding, *J. Lipid Res.* **36**, 211 (1995).
16. M. Dammerman, L. A. Sandkuijl, J. L. Halaas, W. Chung, J. L. Breslow, *Proc. Natl. Acad. Sci. U.S.A.* **90**, 4562 (1993); Q. Zeng *et al.*, *Hum. Genet.* **95**, 371 (1994).
17. M. R. Hayden *et al.*, *Am. J. Hum. Genet.* **40**, 421 (1987).
18. G. M. Dallinga-Thie *et al.*, *J. Lipid Res.* **37**, 136 (1996).
19. W. W. Li *et al.*, *J. Clin. Invest.* **96**, 2601 (1995).
20. B. Staels *et al.*, *ibid.* **95**, 705 (1995); S. Haubenwallner *et al.*, *J. Lipid Res.* **36**, 2541 (1995).
21. S. M. Grundy, A. Chait, J. D. Brunzell, *Arteriosclerosis* **7**, 203 (1987).
22. K. Aalto-Setälä *et al.*, *J. Lipid Res.* **37**, 1802 (1996).
23. Z.-S. Ji, S. Fazio, Y.-L. Lee, R. W. Mahley, *J. Biol. Chem.* **269**, 2764 (1994).
24. N. S. Schacter *et al.*, *J. Clin. Invest.* **98**, 846 (1996).
25. W.-S. Yang, D. N. Nevin, R. Peng, J. D. Brunzell, S. S. Deeb, *Proc. Natl. Acad. Sci. U.S.A.* **92**, 4462 (1995); E. Gagne, J. Genest Jr., H. Zhang, L. A. Clarke, M. R. Hayden, *Arterioscler. Thromb.* **14**, 1250 (1994).
26. K. A. Kieft, T. M. A. Bocan, B. R. Krause, *J. Lipid Res.* **32**, 859 (1991). Diluted samples of pooled plasma from groups of five or six mice were analyzed by using Superose 6 HR column chromatography to fractionate the lipoproteins. Total cholesterol and triglyceride concentrations were determined by enzymatic assay on total plasma or lipoprotein fractions. Separated lipoproteins in the column eluant were quantified by an online column enzymatic assay for cholesterol or by enzymatic assay of individual fractions. All cholesterol profiles are normalized to represent a constant amount of plasma injected.
27. E. M. Rubin, R. M. Krauss, E. A. Spangler, J. G. Verstuyft, S. M. Clift, *Nature* **353**, 265 (1991).

28. We thank L. Royer for help in quantifying APOA1 in α-HDL and pre-β-HDL. APOB transgenic mice were provided by E. R. Rubin. Supported by NIH grants HL 54591 and HL 21006.

11 September 1996; accepted 18 November 1996

Linkage of G Protein–Coupled Receptors to the MAPK Signaling Pathway Through PI 3-Kinase γ

Marco Lopez-Ilasaca,* Piero Crespo,* P. Giuseppe Pellici, J. Silvio Gutkind,† Reinhard Wetzker

The tyrosine kinase class of receptors induces mitogen-activated protein kinase (MAPK) activation through the sequential interaction of the signaling proteins Grb2, Sos, Ras, Raf, and MEK. Receptors coupled to heterotrimeric guanine triphosphate–binding protein (G protein) stimulate MAPK through $G_{\beta\gamma}$ subunits, but the subsequent intervening molecules are still poorly defined. Overexpression of phosphoinositide 3-kinase γ (PI3Kγ) in COS-7 cells activated MAPK in a $G_{\beta\gamma}$-dependent fashion, and expression of a catalytically inactive mutant of PI3Kγ abolished the stimulation of MAPK by $G_{\beta\gamma}$ or in response to stimulation of muscarinic (m2) G protein–coupled receptors. Signaling from PI3Kγ to MAPK appears to require a tyrosine kinase, Shc, Grb2, Sos, Ras, and Raf. These findings indicate that PI3Kγ mediates $G_{\beta\gamma}$-dependent regulation of the MAPK signaling pathway.

The muscarinic receptor m2 was expressed in COS-7 cells together with an epitope-tagged MAPK (HA-ERK2) (*1*). Treatment of cells with the agonist carbachol induced activation of MAPK, and wortmannin, an inhibitor of phosphoinositide 3-kinases (PI3Ks), nearly abolished this effect (Fig. 1A). Furthermore, MAPK activation induced by transient expression of $G_{\beta\gamma}$ or by coexpression of $G_{\beta\gamma}$ and the guanine nucleotide exchange factor Sos was also inhibited by wortmannin (Fig. 1B). In contrast, no effect of wortmannin was observed when MAPK was stimulated by epidermal growth factor (EGF); by a mutationally activated form of MEK, MEK E; or by a membrane-targeted form of Sos, myrSos (Fig. 1, A and B). These results support an essential role for wortmannin-sensitive PI3K in signal transduction from G protein–coupled receptors to MAPK (*2*), separately from the EGF signaling pathway and upstream of Sos and MEK.

Several species of PI3K have been cloned and characterized. Heterodimeric PI3Kα and PI3Kβ, consisting of p110 catalytic subunits and different p85 adapter molecules, are regulated by receptors with intrinsic or associated tyrosine kinase activity (*3*). Another PI3K isotype, termed PI3Kγ, can be activated in vitro by both α and βγ subunits of heterotrimeric G proteins but does not interact with p85 (*4*). We expressed the α and γ forms of PI3K in COS-7 cells and investigated their ability to induce MAPK activity (Fig. 2, A and B). PI3Kγ induced a concentration-dependent stimulation of MAPK. In contrast, expression of PI3Kα or a mutant of PI3Kγ lacking lipid kinase activity, PI3Kγ K799R (*5*), did not affect MAPK activity (Fig. 2, B and C). Stimulation of MAPK by overexpression of PI3Kγ (*5*) was abolished by wortmannin (Fig. 2C). These observations indicate that PI3Kγ may mediate the wortmannin-sensitive activation of MAPK by receptors linked to heterotrimeric G proteins.

We found that expression of the mutated PI3Kγ that lacks lipid kinase activity

M. Lopez-Ilasaca and R. Wetzker, Max Planck Research Unit Molecular Cell Biology, Medical Faculty, University of Jena, 07747 Jena, Germany.
P. Crespo and J. S. Gutkind, Molecular Signaling Unit, Oral and Pharyngeal Cancer Branch, National Institute of Dental Research, Bethesda, MD 20892, USA.
P. G. Pellici, Istituto di Medicina Interna e Scienze Oncologiche, Laboratorio di Biologia Moleculare, Polclinico Monteluce, University of Perugia and European Institute of Oncology, Via Ripamonti 435, 20141 Milan, Italy.

*These authors contributed equally to this work.
†To whom correspondence should be addressed at the Molecular Signaling Unit, Oral and Pharyngeal Cancer Branch, National Institute of Dental Research, National Institutes of Health, 9000 Rockville Pike, Building 30, Room 212, Bethesda, MD 20892–4330, USA.